*Tellus (1995), 47A, 733–746*
*Printed in Belgium – all rights reserved*


**TELLUS**
*ISSN 0280–6495*

# The seclusion intensification of the New Year's day storm 1992

By SIGBJØRN GRØNÅS, *Geophysical Institute, University of Bergen, Allégaten 70, 5007 Bergen, Norway*

(Manuscript received 5 September 1994; in final form 12 December 1994)

ABSTRACT

The Bergen School meteorologists realized that not all cyclones follow their conceptual cyclone model. In particular they found cases with re-generation of occluded cyclones. In their literature, for instance as found in Godske and co-workers, 2 kinds of re-generation were considered challenging to weather forecasting: a thermodynamic intensification with similarities to the development of tropical cyclones, and intensification of what was called the non-frontal trough, or the back-bent occlusion, of strong cyclones. It has been believed that the latter kind is characteristic of the strongest surface winds observed in the Northwestern Atlantic. In this paper such a case, resulting in the strongest cyclone landfall on the Norwegian west coast this century, has been investigated from a simulation of a small synoptic-scale ($\sim$1000 km), fast-moving extratropical cyclone ($\sim$25 m s$^{-1}$). It is found that the cyclone evolves as the conceptual frontal model of Shapiro and Keyser (1990), and that the strong winds are developed by a secondary, mesoscale ($\sim$500 km) cyclogenesis closely linked to the seclusion process. The time scale of the intensification is 12 h, starting with what is called the seclusion trough at the tip of the back-bent warm front. As the cold air secludes the warm core, the disturbance develops into a separate low, here called the seclusion low. Release of latent heat connected to the back-bent warm front is found to play an important role in forming the seclusion. A part of the generated potential vorticity (PV) remains within the warm air in the seclusion process. Inversion of the low-level PV anomalies results in a low-level jet along the outer side of the seclusion trough. The strong winds are observed when the seclusion trough develops into the seclusion low and the low-level jet becomes parallel to the large scale westerly flow. A positive PV anomaly streamer, formed from a larger scale upper PV anomaly in phase with the surface low, takes part in this stage of the development.

## 1. Introduction

During the occlusion process of an extratropical cyclone, available energy is gradually consumed and the cyclone normally enters a de-generation process. For various reasons, however, an occluded cyclone might enter a new period of intensification. The Bergen School meteorologists mentioned several kinds of such re-generation (e.g., Chromow and Koncek, 1940, p. 357; Godske et al., 1957, p. 743). Two kinds were considered a challenging problem of weather forecasting: a thermodynamic intensification with similarities to the development of tropical cyclones, and an intensification of what they called the non-frontal trough in the cold air, or the back-bent occlusion, defined as an extension of the occlusion backwards (normally towards southwest) into the non-frontal trough (Godske et al., 1957, p. 537).

The thermodynamic re-generation was studied by Bergeron (Bergeron, 1949; Bergeron, 1954; see also Godske et al., 1957, p. 734), who claimed that such developments take place in "a true tropical hurricane style" in certain extratropical regions during late summer and early autumn. According to Bergeron, such re-generations might form on the occlusion of a pre-existing cyclone of ordinary intensity. A mesoscale, near-symmetrical low-level disturbance is formed, with a diameter generally less than 500 km, causing strong wind and

heavy precipitation. Developments of this kind have been simulated numerically and discussed by Kristjansson (1990) and Grønås et al. (1994). In these cases organised release of latent heat, within 12 h, concentrated a strong, low-level, near symmetrical anomaly of potential vorticity (PV) below the heat source, and a minimum anomaly above. In this way a warm disturbance (diameter 2–300 km) was created with cyclonic inflow near the surface and anticyclonic outflow aloft. According to Grønås et al. no high-level positive PV anomaly was involved in this first stage of the development.

This paper is devoted the study of the intensification of the non-frontal trough in the cold air (or the back-bent occlusion). It was believed that such secondary developments are connected to the occlusion of strong cyclones. It was further assumed that the re-generation is influenced by divergence aloft resulting from an unstable upper wave. A clear understanding of the non-frontal trough (or the back-bent occlusion) intensification was not obtained by the Bergen School meteorologists, and a standard way of operational analysis was never introduced. In Norway, some meteorologists used the term non-frontal trough, but the majority used the term back-bent occlusion. The normal procedure for Norwegian meteorologists has been to watch for signs of development connected to the back-bent occlusion in strong cyclones. As a young forecaster in the late 1960s, I was informed that the strongest winds ever recorded in our region have been linked to back-bent occlusions. Such a structure has been called "the poisonous tail" of the back-bent occlusion (after F. Spinnangr, who in 1939 succeeded S. Pettersen as head of the Western Norway Forecasting Office). Later Andersen (1978) investigated several cases with such development on the basis of conventional observations and satellite images. He found that the intensification normally is connected to what he called the inner part of rolled-up occlusions. He pointed out that the tendency for occlusions to be arranged in a spiral pattern in intense cyclones was known by the Bergen School meteorologists (Godske et al., 1957, p. 537), and referred also to Scherhag (1969) for pointing out the significance of warm-air advection of such rolled-up occlusions.

Based on air-craft measurements Shapiro and Keyser (1990) more recently documented interesting mesoscale ($\sim$150–400 km) structures in rapidly developing marine cyclones. In particular, during the mature phase polar air completely encircles the centre, secluding a warm pocket of low level air (below 700 hPa) near the low centre. In the stages prior to the seclusion they found no occlusion process, but a back-bent warm front north of the cyclone perpendicular to the cold front. This feature and the seclusion of warm air are not contained in the classical Norwegian cyclone model, and Shapiro and Keyser proposed a new conceptual cyclone model for the life cycle of rapidly developing cyclones. It is interesting to note that their findings have been suggested in idealized numerical simulations (Hoskins and West, 1979; Schär, 1989; Schär and Wernli, 1992). In particular, these studies show that the seclusion process can take place without diabatic heating.

The findings of Shapiro and Keyser raise a number of questions concerning the evolution of fronts in the life cycles of extratropical cyclones, questions which now are being debated in the meteorological literature. A hypothesis of this paper is that the seclusion process in some cases describes what earlier was called the intensification of the nonfrontal trough. If so, the seclusion must be followed by a rapid, mesoscale cyclogenesis causing strong winds at the surface. If such an intensification follows the seclusion process, it is important to understand this secondary cyclogenesis, for instance to investigate the role of upper and lower disturbances, and the role of latent heating.

The limited conventional data available over ocean can not resolve the seclusion process. In this paper a high-resolution numerical simulation of an observed case reproduced major features of a rapid, vigorous cyclogenesis. In addition, an intensification at the normal position of the nonfrontal trough gave extreme strength of the surface winds. These winds could also be said to be connected to a mesoscale cyclogenesis through the seclusion process. It is believed that the study of the data provided by the numerical simulation gives useful insight into the issues raised above. The case chosen is the New Year's day storm 1992, an exceptional strong cyclone resulting in the strongest storm recorded in Norway this century, striking the coast of Norway north of Bergen (Aune and Harstvedt, 1992). In Section 2 the numerical experiments are described and verified. The frontal structure and in particular the seclusion process is shown

in Section 3. In Section 4, the surface pressure tendencies of the secondary development are presented together with the surface winds. The main cyclogenesis and the effect of latent heat release are described in Section 5 and a further description of the intensification/seclusion is given in Section 6 using a PV analysis.

## 2. The numerical simulations

On 1 January 1992, the west coast of Norway north of Bergen experienced hurricane-force winds. Maximum observed mean wind speed was 46 m $s^{-1}$ at 2 lighthouses (Svinøy and Skalmen, Møre County). The storm caused the largest natural disaster in Norway in modern time, but no human lives were lost. The storm was successfully forecasted by the Norwegian Meteorological Institute (DNMI) from numerical prognoses from European Centre for Medium Range Forecasting (ECMWF).

Simulations of the storm have been made with the DNMI numerical model (Grønås and Hellevik, 1982; Grønås et al., 1987; Nordeng, 1986; Grønås and Midtbø, 1987). The stereographic integration area with $121 \times 97$ points has been adapted to cover the track of the storm. The grid length has been 50 km at 60°N, with 18 levels between 100 hPa and surface. The initial analyses of wind, geopotential height, and relative humidity on 10 pressure levels have been taken from ECMWF, and ECMWF analyses every 6 h have been used as lateral boundary conditions. Sea surface temperature (SST) has been taken from subjective analyses from DNMI. The extension of the model to include the hydrological cycle according to Sundqvist et al. (1989) has been applied. It includes a prognostic equation of liquid water and some refined microphysical processes connected to the precipitation processes. The Norwegian model with the so-called Sundqvist scheme has shown to give better results than the operational condensation scheme in cases of mesoscale cyclogenesis, when release of latent heat plays a major role (Kristjansson, 1990; Grønås et al., 1994).

The storm has also been simulated by Breivik et al. (1992) using the same model, but on another integration area and with the operational condensation scheme (Nordeng, 1986). They made a large number of sensitivity experiments related to diabatic effects, air-sea interaction, initial conditions and condensation schemes (standard condensation scheme, Sundqvist scheme and certain parameters in the operational scheme). They found that the mesoscale structures of the storm were best simulated by the Sundqvist scheme. Release of latent heat had a major effect on the cyclogenesis. In comparison, air-sea interaction played a minor rôle.

Two experiments with the Sundqvist scheme have been performed: one control run and one run where latent heat of condensation has been removed. Both runs were integrated for 42 h. It should be stressed that because of the analyses at the lateral boundaries, the simulations are not predictions, but rather hindcasts, which are much closer to the observations than any operational numerical forecast available at the time when DNMI forecasted the storm.

With the control run a realistic simulation of the cyclone development was obtained, simulating the strong winds at the right place and almost at the correct time. In Fig. 1a is shown the sea level pressure (SLP) and wind speed at the lowest model level ($\sim$40 m) after 30 h integration, when the strongest surface winds were found (0600 UTC 1 January). The surface fronts have been subjectively drawn from the distribution of equivalent potential temperature ($\theta_e$) at 925 hPa. The reanalyzed subjective surface map at the same time from DNMI's Bergen Office, including an analysis of the wind speed, is shown in Fig. 1b. The intense cyclone ($\sim$1000 km) with the strong winds at the position of the non-frontal trough, south-southwest of the low centre in the subjective analysis, is well captured. The analyzed minimum pressure is about 6 hPa lower than in the simulation. The track of the simulated low follows the observed one closely, however, at this time the low is estimated to be 2 h behind the analyzed low.

The fronts on the two maps agree well with respect to the warm and cold front structure south of the low. In the subjective analysis an occlusion is drawn northward to the eastern side of low centre. However, in the simulated cyclone a warm tongue of air has been stretched around the low and down in the position of the non-frontal trough. This tongue has been drawn as a warm front (see Section 3) around the low and extended southward on its tip as a stippled line along maximum $\theta_e$ in the west-east direction. There is a

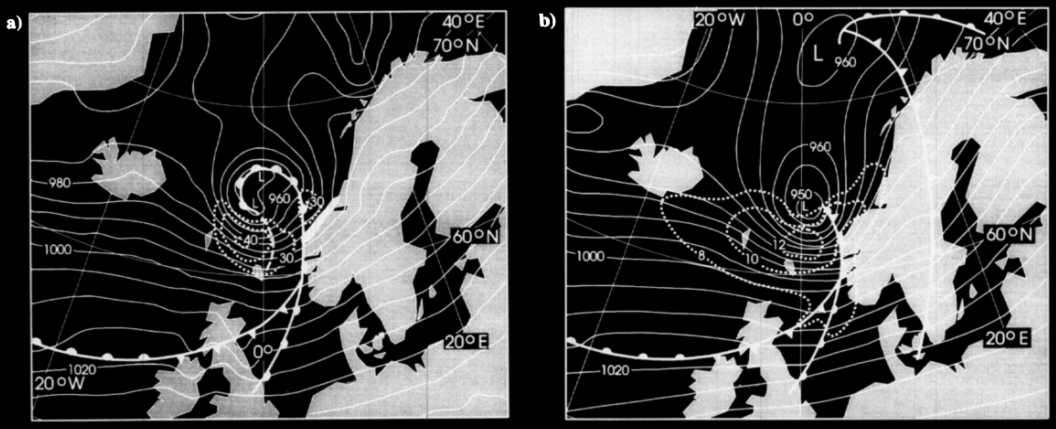


*Fig. 1.* (a) Simulation (30 h) valid 06 UTC 1 January 1992 of SLP (contour step 5 hPa) and wind speed larger then 30 m s$^{-1}$ (contour step 5 m s$^{-1}$) at the lowest model layer (40 m). On the Norwegian coast is marked the area with severe damage. (b) Surface analysis at the same time from DNMI's Bergen Office with fronts, isobars and contours for wind force 8, 10 and 12 on the Beaufort scale.

warm core seclusion ($\sim$150 km) at the tip of the back-bent warm front. Later the warm air inside the warm front and the stippled line was further encircled by colder air to become the inner part of a seclusion on a larger scale (see Section 3 and Fig. 3c).

The way of marking the front in Fig. 1a has often been used by meteorologist (Andersen, 1978), but with an occlusion instead of the back-bent warm front. The alternative indication as in Fig. 1b, without any back-bent structure and just a non-frontal trough, has been preferred by other meteorologists. In our case the back-bent structure is evident, as will be shown in the next section, and the frontal description of the occlusion in Fig. 1b is probably not correct.

An area with wind force 12 on the Beaufort scale is shown at the subjective analysis. Maximum simulated wind in the same area (lowest model level) is 41 m s$^{-1}$, and maximum geostrophic wind is 85 m s$^{-1}$. The strong winds entered the coast of west Norway immediately afterward. The area influenced with widespread damage is shown in Fig. 1a. The strongest simulated winds hit in the middle of this area.

The simulated cyclone centre SLP decreases during a period of 30 hours from 31 December at 00 UTC. The pressure decrease is 52 hPa and the minimum simulated SLP reaches 952 hPa, Fig. 2. The disturbance starts west of New Foundland and its speed northeastward is very high, more than 25 m s$^{-1}$ during the first stages. The simulations have been further compared with re-analyzed, subjective surface analyses from DNMI's Bergen office and in addition, with another independent set from DNMI's Oslo office. There

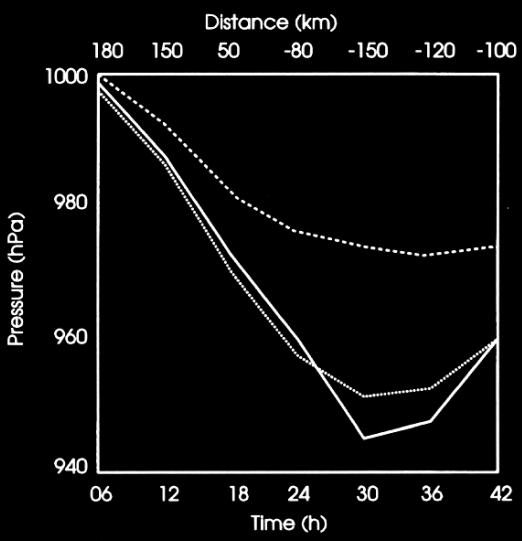


*Fig. 2.* Simulated and analyzed central SLP of the cyclone as a function of time. Dotted line: simulation, heavy line: analyses, stippled line: simulation without release of latent heat. Position errors (km) of the low centre at the top of the figure.

were few observations along the track of the cyclone and the two analyses show some differences both with respect to the depth of low and the positions of the fronts. The minimum analyzed SLP pressure is 945 hPa, occurring at the same time as in the simulation (30 h). The difference of 5–7 hPa between the analyses and the simulation is partly due to the flat centre in the simulation. The pressure gradients connected to the belt of maximum winds correspond well with the analyzed pressure gradients. The decaying phase from 30 to 42 h is well simulated.

## 3. The fronts

The development of the storm, shown in Fig. 3, is very well in accordance with the conceptual frontal model of Shapiro and Keyser (1990), and demonstrated by observational case studies (Shapiro and Keyser, 1990; Neiman and Shapiro, 1993 and Neiman et al., 1993) and numerical simulations (Kuo et al., 1992; Del'Osso and Klinker, 1994). Shapiro and Keyser introduced the expression back-bent warm front, which corresponds to what earlier has been called the rolled-up occlu-

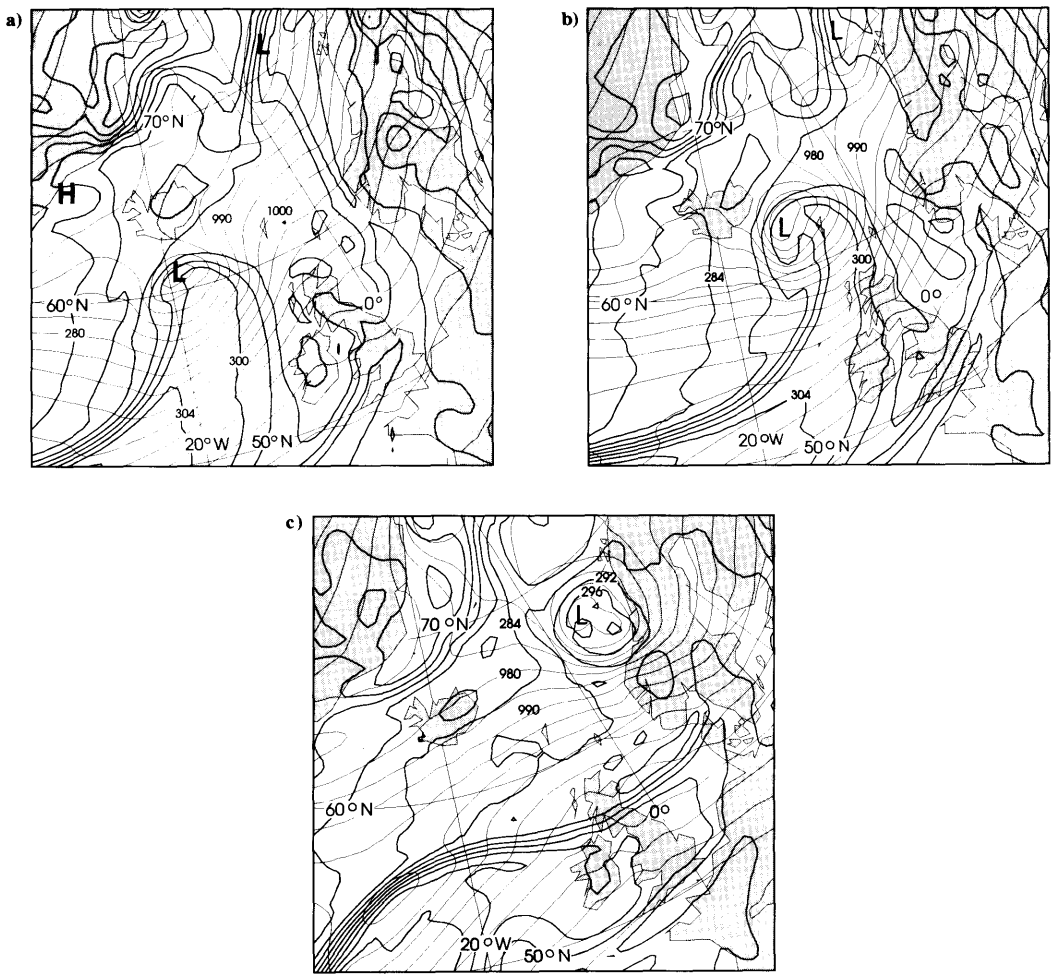


*Fig. 3.* Simulated SLP (thin lines, contour step 5 hPa) and $\theta_e$ at 925 hPa (thicker lines, contour step 4 K). (a) 18 h, valid 18 UTC 31 December 1991. (b) 24 h, valid 00 UTC 1 January 1992. (c) 36 h, valid 12 UTC 1 January 1992.

sion. (The back-bent warm front should not be related to what the Bergen School meteorologists called the back-bent occlusion). Within a period of 36 h the cyclone develops through the four stages: the nascent frontal cyclone, the frontal fracture stage, when the cold front looses contact with the warm front, the frontal T-bone stage with the back-bent warm front, and at last the stage of warm core seclusion. The nascent stage took place east of New Foundland, more than 2500 km away from the Norwegian coast. Already at this stage the surface front is strong (not shown). This is a minor difference to the Shapiro/Keyser conceptual model, which shows a wider area with strong baroclinicity. The development of the back-bent warm front is clear and connected to a tongue of warm air being wrapped around the low. This front is close to perpendicular to the cold front, and no classical occlusion process, where the cold front overtakes the warm front, can take place in this area. In this way the expression "rolled-up occlusion" is here not correct.

From 18 h into the integration the cyclogenesis is characterized by the seclusion process in which warm air is surrounded entirely by cold air. As already mentioned, the warm core is found at the southern side of the low just north-northeast of the strong winds. After 24 h (Fig. 3b) this seclusion is not completed, but a warm anomaly (scale $\sim$150 km) is found in the position of the trough south of the low. The structure is similar to that found by Shapiro and Keyser (1990), Neiman et al. (1993) in their ERICA IOP-4 storm. Northeast of the low centre another more elongated warm anomaly is found. After 36 h these two disturbances have been merged into one, rather circular anomaly (Fig. 3c). The merging of the two anomalies takes place in a decaying phase of the cyclone after the intensification. The diameter of the warm anomaly is 500 km with an amplitude of 6 K in temperature and 12 K in $\theta_e$. This is a similar structure as measured by Shapiro and Keyer (1990) in their mid-Pacific case. The two warm anomalies are found below 600 hPa. After 36 h the large anomaly is apparent below 850 hPa. Above 850, there are still two warm anomalies with cold air in between, encirculating the southernmost anomaly.

The secluded warm air is warmer than indicated by the conceptual model. Some trajectories (not shown), computed backwards from the secluded warm air, tend to go back to the warm side of the front in the nascent stage. Warm air is also indicated by the temperature distribution. The maximum $\theta_e$ in the seclusion at 925 hPa after 36 h is 301 K. In the beginning of the simulation the 301 K contour is one of the contours defining the frontal zone east of New Foundland.

The warm front on the eastern side of the low at 18 and 24 h is sloping eastward in a normal way, but the back-bent warm front is steep toward north and the vertical stability is low (Fig. 9a, b). A branch of the dry intrusion (Browning, 1990) in the rear of the cyclone overtakes the cold front (not shown), which is shallow, tilting westward above the boundary layer, but with the characteristic change to a easterly tilt close to the surface (Thorpe and Clough, 1991). During the seclusion process, the cold air-masses are dominating and the stability is low in the lower part of the troposphere (below 550 hPa). At the tip of the back-bent warm front and at the edge of the secluded warm air, the contours of the equivalent potential temperature ($\theta_e$) are close to vertical in the lower troposphere (see Fig. 9b, c).

After 30 h the cold front south of the cyclone overtakes the warm front and an ordinary occlusion is formed. After 36 h, when the seclusion is completed, this occlusion extends northward over eastern Scandinavia from a triple point over Denmark. The occlusion is not in accordance with the Shapiro/Keyser model.

## 4. Pressure tendencies and surface winds

As indicated in Fig. 1 and Fig. 3c, the simulation shows two separate low centres when the storm makes landfall at the coast of Norway. During the first three stages of the frontal evolution, the SLP tendencies, computed relative to the translation speed of the cyclone centre, have their largest pressure decrease concentrated at the centre of the cyclone (Fig. 4a). The strongest surface winds are found in the warm air and along the warm front. When the seclusion process begins after 18 h of integration, a secondary intensification takes place at what was called the non-frontal trough, but also at the back-bent warm front ahead of the low centre (Fig. 4b). The expression "non-frontal trough" is here not correct. The trough is closely connected to the back-bent warm front and the

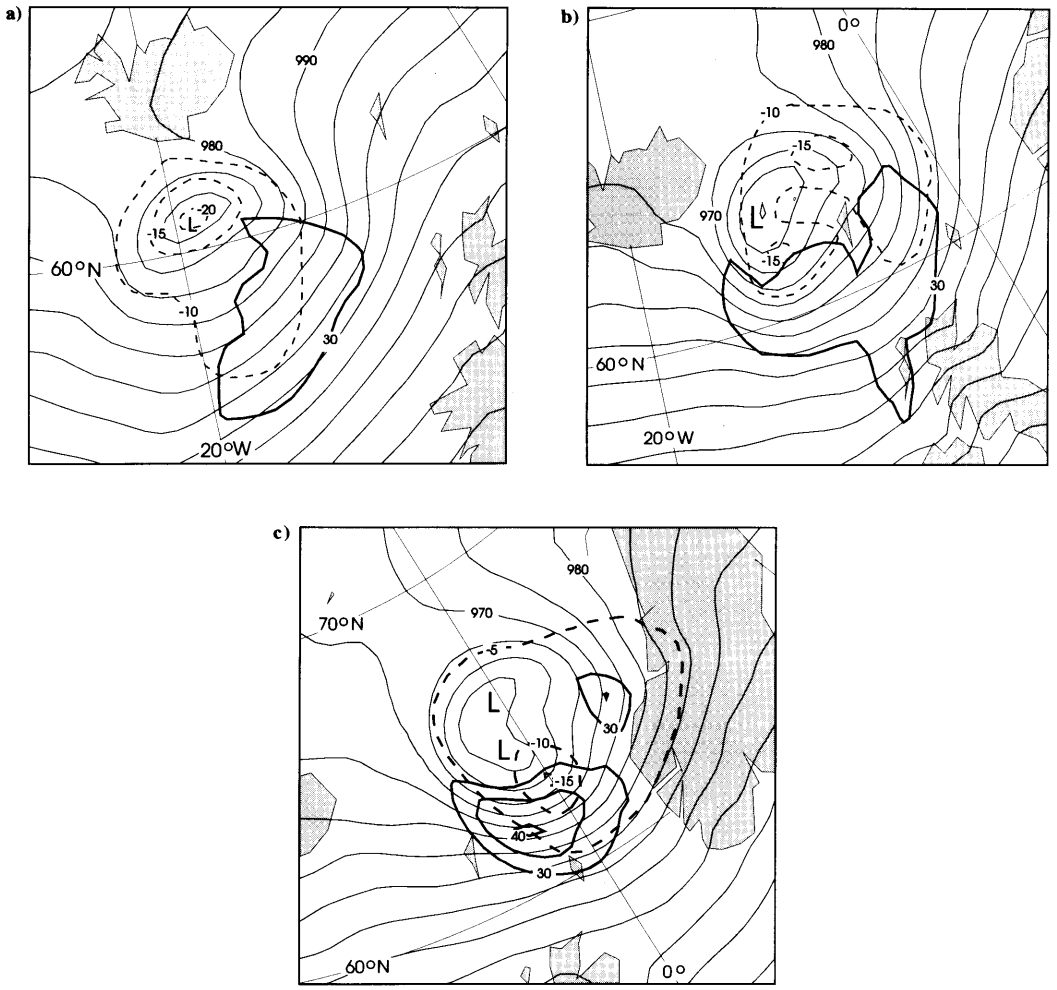


*Fig. 4.* Simulated SLP (contour step 5 hPa), 6 h SLP tendencies relative to the cyclone (stippled lines, contour step 5 hPa in 6 h), and wind at lowest model layer above 30 m s$^{-1}$ (thick lines, contour step 5 m s$^{-1}$). (a) 18 h valid 18 UTC 31 December 1991. (b) 24 h valid 00 UTC 1 January 1992. (c) 30 h valid 06 UTC 1 January 1992.

seclusion process, and will be called the seclusion trough. Two new mesoscale lows are being generated within 12 h (from 18 to 30 h) on the flanks of the original low resulting in two separate low centres. The minimum SLP of the total cyclone does not decrease significantly during the process.

The deepening of the seclusion trough results in what will here be called the seclusion low. The total pressure decrease at the surface is close to 30 hPa and a typical horizontal scale is ~500 km. After 6 h of development (24 h simulation), the seclusion trough is pronounced. Strong surface winds are now found at both sides of the trough. Six hours later (Fig. 4c) the seclusion cyclone has developed into a more circular shape. The wind increases significantly during this process (10 m s$^{-1}$ in 6 h) and reaches exceptional values (41 m s$^{-1}$). In this process both the pressure gradients and the radius of curvature of the disturbance increase. This development surely demonstrates "the poisonous tale" and the intensification that Bergeron urged the forecasters to watch out for.

## 5. The main cyclogenesis and the effect of latent heat release

Comparison of the two integrations with and without release of latent heat of condensation shows that released heat greatly affects the development. As seen from Fig. 2 the added heat strengthens the low from the beginning of the development, 22 hPa of the maximum pressure drop of 52 hPa is caused by this effect. Although large, this heatening effect is less than simulated in some other explosive developments. Kuo and Reed (1988) found that half of the development was caused by latent heat release in an explosive development in the eastern Pacific. For the "October Storm" over England in 1987, Shutts (1990) found that two third of the development was due to diabatic processes.

The main cyclogenesis is a baroclinic development in accordance with the cyclogenesis model of Hoskins et al. (1985). As in their model the cyclogenesis can be explained as a mutual interaction of an upper air PV anomaly and a surface temperature anomaly. The vertical coupling between the anomalies is known to be proportional to the Rossby height, which is inversely proportional to the vertical stability expressed by the Brunt-Väisälä frequency, proportional to the scale of the disturbance and an effective Coriolis parameter. In addition comes the effect of added heat and friction.

In the beginning of the integration the baroclinicity is concentrated in a narrow frontal zone through the troposphere with a broad jet (maximum speed 75 m s$^{-1}$ at 300 hPa). The development starts in a classical way at the entrance of the jet. A folding of stratospheric PV is connected to the left entrance and a nascent surface wave below the right entrance (not shown).

The evolution of the surface temperature wave has been shown earlier (Fig. 3). The upper PV anomaly has been studied from isentropic maps and maps of $\theta$ in PV surfaces. Maps of PV at the 300 K surface are representative for the upper PV anomaly folded down from the stratosphere. Fig. 5 shows the PV distribution at this surface after 24 h. A distinct, positive anomaly with a maximum of 3.5 PVU and a scale $\sim$500 km is connected to the low. The PV maximum is well conserved during the development, but the anomaly grows in strength, descends from 425 hPa at 6 h to 520 hPa

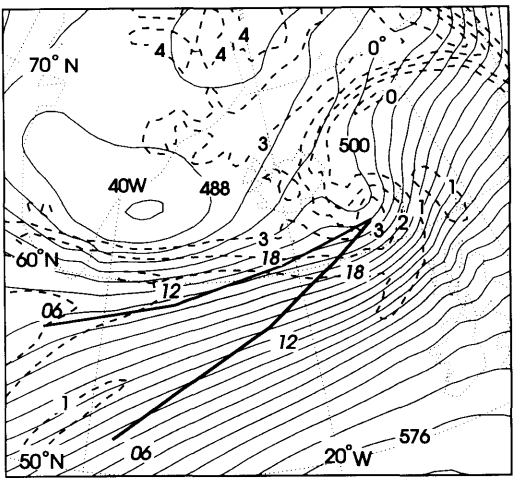


*Fig. 5.* Simulated PV at the isentropic surface 300 K after 24 h (stippled lines, contour step 1 PVU) and geopotential height at 500 hPa (contour step 40 m), valid 00 UTC 1 January 1992. The tracks of the PV anomaly at this isentropic surface and the anomaly of temperature at 925 hPa are drawn in thick lines.

at 24 h and moves rapidly toward east-northeast (speed $\sim$25 m s$^{-1}$). The PV structure extends far down in the troposphere, for instance the 2.5 PVU surface reaches 600 hPa after 24 h (see cross-section Fig. 9b). After 24 h, the upper PV anomaly and the surface temperature anomaly are in phase. Tracks of the temperature anomaly at the surface and the PV anomaly aloft are marked in Fig. 5. The two anomalies act together in a normal way from a rather large tilt after 6 h (horizontal distance $\sim$750 km).

Following Hoskins et al. (1985), Hoskins (1990), Thorpe and Clough (1991), and assuming a vertical vorticity vector, the effect of latent heat released by condensation can also be described to concentrate a positive anomaly of PV below the heat source and a negative anomaly above. The normal effect of this on the cyclogenesis process is to strengthen the cyclone near the surface (see Section 6) and the upper-tropospheric ridge (Uccellini, 1990; Davis et al., 1993). The latter has a major cyclogenetic effect in our case, since the low PV air-masses are being wrapped around the upper positive PV anomaly. This is seen from Fig. 6, which shows the PV structure at 300 K after 30 h in the integrations with and without latent heat release. For vertical distribution see also

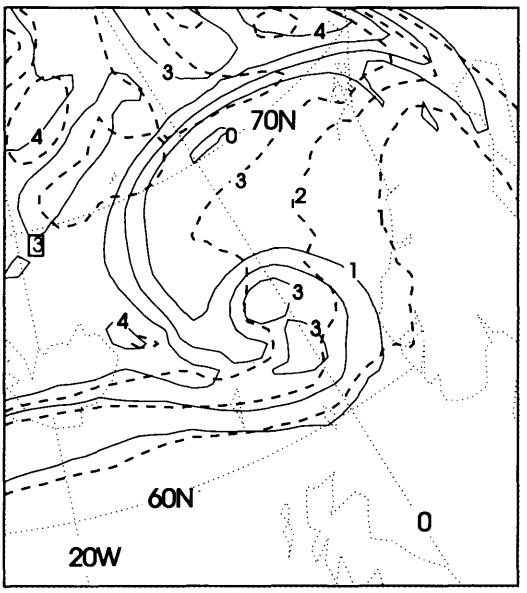


*Fig. 6.* Simulated PV at the isentropic surface 300 K after 30 h (continues lines, contour step 1 PVU) and PV at the same surface when release of latent heat is excluded (stippled lines).

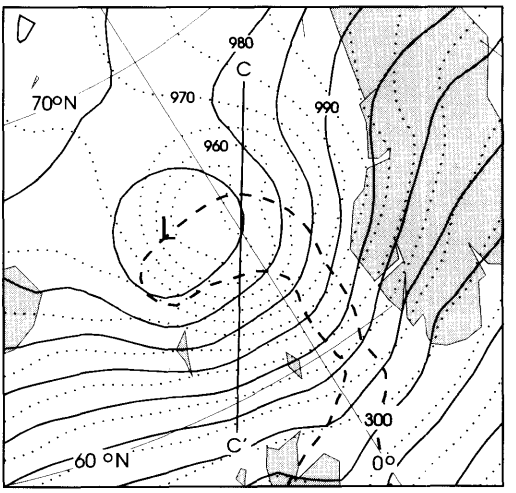


*Fig. 7.* Simulation (30 h) without latent heat release, valid 06 UTC 1 January 1992. Heavy lines: SLP (contour step 5 hPa), stippled line: 300 K contour of $\theta_e$ at second lowest model level. For reference SLP (dotted lines, contour step 5 hPa) from the standard run is shown.

cross-sections in Fig. 9b, c, d, where d is a cross-section through the occlusion in the dry case. The wrapping of low PV air on the northern side strengthens the positive anomaly considerably. Without latent heat release the anomaly is much weaker and takes a trough-like structure. The wrapping of low PV air on the northern side of the cyclone is missing.

A characteristic of the intense cyclone is its small upper scale, which is similar as the scale of the surface low. This can be seen from the map of geopotential height after 24 h in Fig. 5. The scale is estimated to 800 km, measured between the ridges on each side. The small scale is connected to the saturated ascent found in advance of the cyclone which reduces the stability and increases the Rossby height. Generally this results in tighter vertical coupling, tighter phase locking, more mutual amplification, and much faster development on smaller spatial scales.

The seclusion process takes place beneath the upper air PV anomaly where the vertical stability is generally low (Hoskins et al., 1985). This explains the low lower-tropospheric vertical stability mentioned earlier in the air-masses taking part in the seclusion (see contours of $\theta_e$ in cross-sections through the secluded air in Fig. 9c). In this way the vertical coupling is high between the upper PV anomaly and the warm anomalies contained in the cold air. Rapid intensifications, as shown in the former section, might take place.

These mesoscale developments, both ahead of the low and at the seclusion trough/low, are missing when latent heat is excluded, Fig. 7. The exceptional strong surface winds are absent, e.g., maximum geostrophic wind is reduced to half of its strength. It is also seen from the figure and Fig. 6 that the translation speed of the low is reduced without the added heat. Normally an increase in the development slows down the translation speed of a cyclone (Hoskins et al., 1985), but in this case the main jet has become stronger.

## 6. PV analysis of the seclusion

The largest amounts of precipitation are found on the warm front ahead of the cyclone and north of the low at the back-bent warm front. Maximum rates are close to 4 mm an hour during the strongest development. The added heat results in a positive low-level PV anomaly concentrated below

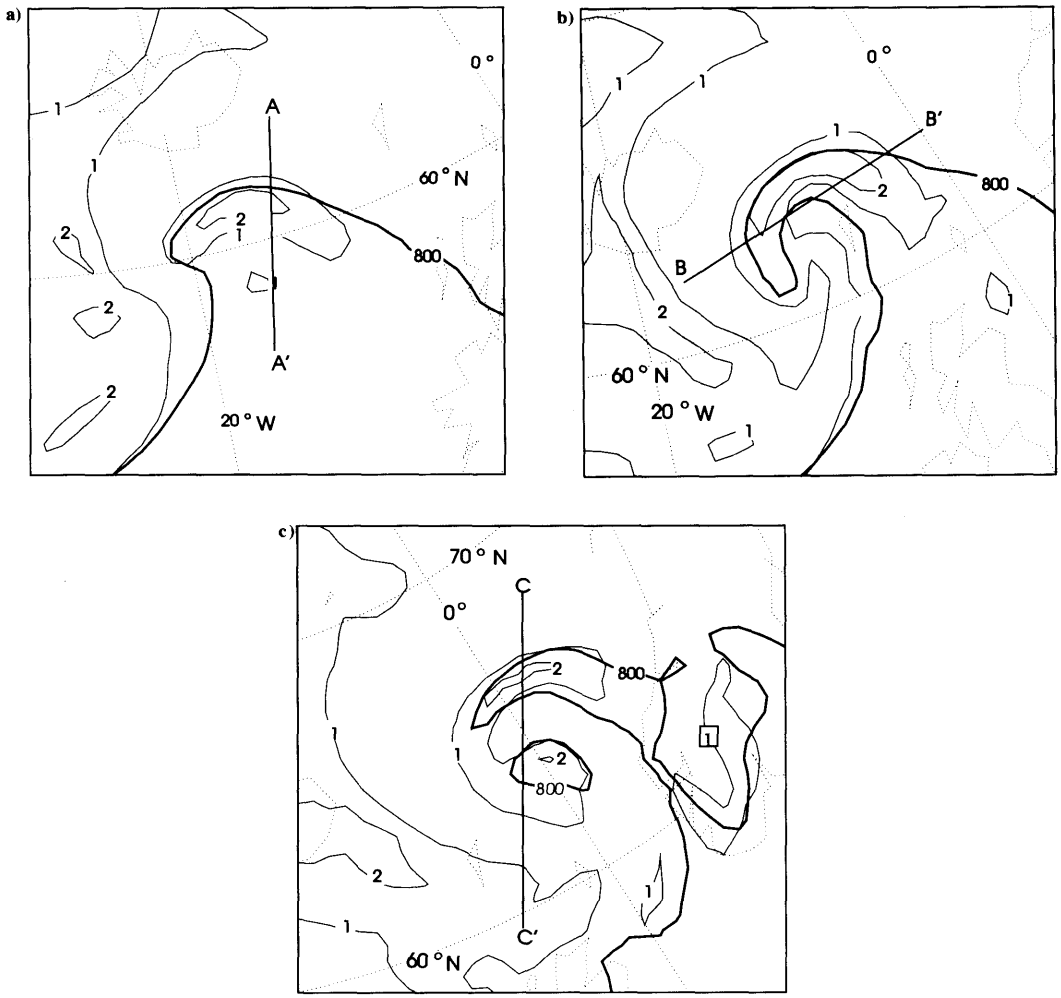


*Fig. 8.* Simulation of PV at the isentropic surface 287.5 K (contour step 1 PVU). Heavy line: 800 hPa contour of the height of the isentropic surface. Positions for cross-sections in Fig. 9 are shown. (a) 18 h valid at 18 UTC 31 December 1991. (b) 24 h valid at 00 UTC 1 January 1992. (c) 30 h valid at 06 UTC 1 January 1992.

the heat source. After 18 h an elongated structure with a maximum value of 2.5 PVU at 800 hPa is connected to the back-bent warm front. This is seen in the PV distribution in the 290 K surface in Fig. 8a and the cross section in Fig. 9a. The PV structure has been stretched along the warm tongue of air of the back-bent warm front. This gives a simple reinforcement effect of the PV anomaly and the anomaly of the surface temperature. Inversion of the anomalies results in a low-level jet on the outer side of the back-bent warm front. This jet is shown in the cross-sections in Fig. 9a, b. Maximum wind speed of 22 m s$^{-1}$ is found at ~925 hPa at 18 h.

The warm air with the PV anomaly is being advected around the cyclone as shown by the wind relative to the cyclone (not shown). In this process the surface temperature and the PV structure are in phase. The largest PV anomalies caused by latent heat release are found 6 h later. Now the seclusion trough has been formed. The structure of the trough is shown by the isentropic map in

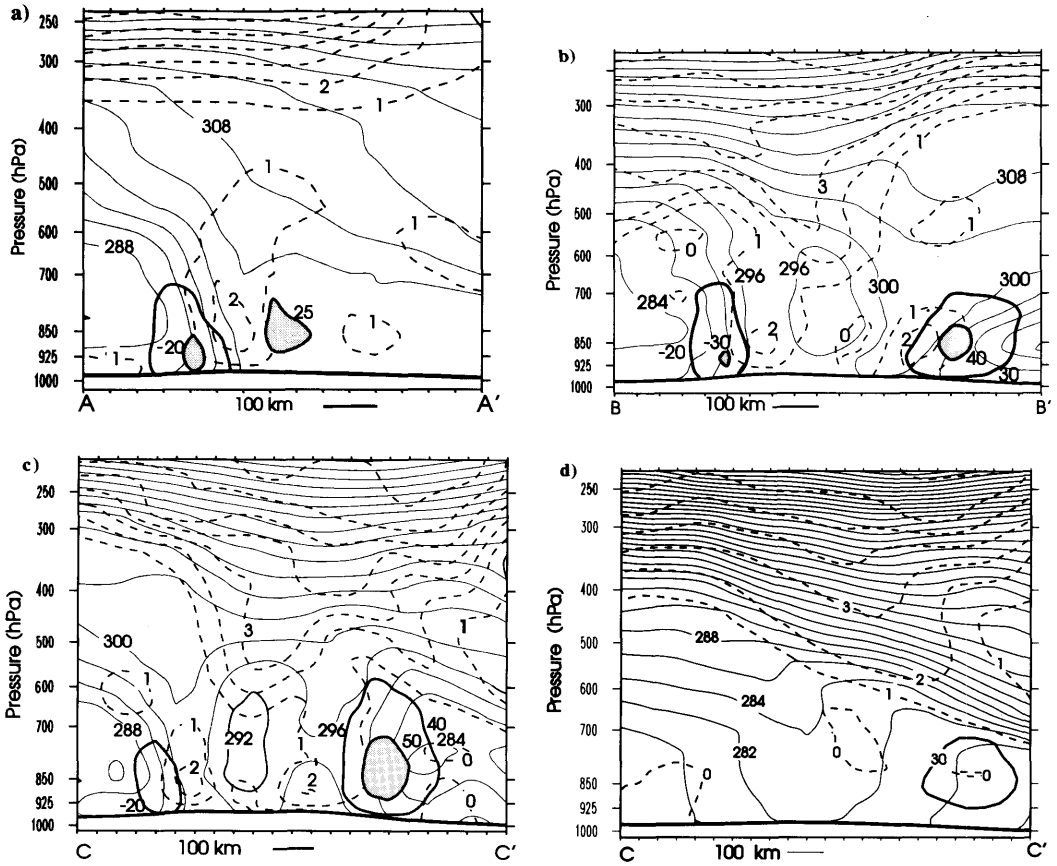


*Fig. 9.* Cross-sections through the simulated cyclone at positions shown in Fig. 8. Continuous thin lines: $\theta_e$ (contour step 4 K). Stippled lines: PV (contour step 1 PVU). Positions of the low-level jets are marked with selected isotachs (contour step 10 m s$^{-1}$). (a) 18 h valid at 18 UTC 31 December 1991, for position see (a). (b) 24 h valid at 00 UTC 1 January 1992, for position see (b). (c) 30 h valid at 06 UTC 1 January 1992, for position see (c). (d) same position as in (c), but $\theta$ and PV when release of latent heat is excluded. In lower right is shown one contour (heavy line) of the normal wind component of the low-level jet. Maximum speed of the jet is 32 m s$^{-1}$.

Fig. 8b and the cross-section in Fig. 9b. The low-level jet at this time obtains northerly winds of 30 m s$^{-1}$.

The seclusion of the warm anomaly is completed during the next 6 h. After 30 h, the cold air has secluded the warm air as shown by the isentropic map in Fig. 9c, where the contour of 800 hPa indicates the low-level warm anomaly, and the cross-section in Fig. 9c. The warm anomaly has been advected further around the main low. Now the inverted winds from the secluded structure are parallel with the general westerly flow on the southern side. The large wind speeds (60 m s$^{-1}$) of the low-level jet (core at 850 hPa, diameter ~250 km) might then be explained as a superimposition of the larger scale wind and the wind generated by the seclusion disturbance.

As seen from the cross-sections Fig. 9b, c, the upper level PV structure penetrates far down towards the cold air northeast of the secluded warm air. Does this PV structure play an active role in the seclusion intensification, or could the development be explained by inversion of the PV anomalies within the secluded warm air? We have earlier explained that the air-masses involved have very low stability and that conditions for mutual interaction are favourable. Indeed, a streamer of positive anomaly PV (diameter ~250 km, ampli-

tude 1.5 PVU) is extending down from the main upper PV anomaly. This is shown at the isentropic map in Fig. 6 and at the cross-section through the seclusion in Fig. 9c. At low levels this anomaly is merged with the PV anomaly (2 PVU at 925 hPa) contained in the seclusion and mentioned above. The low-level jet has grown into a deeper vertical and larger horizontal scale as indicated above. The strengthening of the low-level jet and the formations of the PV anomaly streamer took place during six hours, and acted together with the low-level anomalies within the warm core in the latest stage of the seclusion.

## 7. Concluding remarks

The Bergen School meteorologists considered what they called the non-frontal trough intensification of strong cyclones, or the back-bent occlusion intensification, a meteorological phenomenon causing exceptionally strong surface winds and a challenging forecasting problem. Norwegian forecasters have carefully watched for such developments in daily forecasting, and sometimes referring to this phenomenon as "the poisonous tail of the back-bent occlusion". To the author's knowledge the occurrence of such "tails" have not been estimated. For waters of northwestern Europe, a guess is that cases with force 12 on the Beaufort scale occur nearly every winter. The latest winters have been exceptionally stormy and several cases could be found.

A case, which might be classified as such a development, has been studied from a realistic simulation of a strong extratropical cyclone. Analysis of the simulation shows that the frontal development of the storm evolves according to the conceptual frontal model proposed by Shapiro and Keyser (1990). The formation of the back-bent warm front and the following seclusion process is well defined. The warm core of the seclusion has a diameter of $\sim 150$ km and is found below 600 hPa. In the decaying phase of the cyclone this small-scaled anomaly merges with a warm anomaly ahead of the low to a shallow seclusion on a larger scale ($\sim 500$ km). Two features of the frontal development do not follow the Shapiro/Keyser model: At the time when the seclusion is completed, an ordinary occlusion, where the cold front overtakes the warm front, develops south of the low. The secluded air is warmer, and might have originated from the warm tropical air mass taking part in the cyclogenesis.

When the warm air is being secluded by cold air, the cyclone intensifies through a mesoscale lower-tropospheric cyclogenesis. The development is here called the *seclusion intensification* resulting in the *seclusion low*. It develops within 12 hours from what is here called the *seclusion trough* being formed at the tip of back-bent warm front. The seclusion trough corresponds to what was earlier called the non-frontal trough or the trough of the back-bent occlusion. The surface pressure decrease connected to the seclusion low is $\sim 30$ hPa and a horizontal scale is estimated to 500 km. The seclusion trough and the seclusion low develop a low-level jet. Maximum wind speed of the jet (60 m s$^{-1}$ at 850 hPa) is found in the cold air on the southern side of the seclusion low. The strong westerly winds might be seen as a superimposition of the jet of the mesoscale seclusion low and the larger-scale flow.

The main cyclone (scale $\sim 800$–1000 km through the troposphere) develops within 30 h according to the dynamical cyclone model of Hoskins et al. (1985), as interaction between an upper air PV anomaly, folded down from the stratosphere at the left entrance of the jet, and a temperature anomaly at the surface below the right entrance of the jet. The cyclogenesis is strong (52 hPa in 30 h in the simulation) and the cyclone fast-moving (25 m s$^{-1}$). Large amounts of precipitation ($\sim 4$ mm an h) are found ahead and north of the low along the back-bent warm front. The released latent heat strengthens the cyclone considerably. The upper PV anomlay is increased substantially when low PV air, concentrated above the heat source, is being advected around the anomaly. In addition, the cyclone is intensified by a significant low-level PV anomaly concentrated below the heat source.

Two conditions of dynamical nature have been found to be important for the seclusion intensification. The first is the distinct low-level PV anomaly being formed along the tongue of warm air connected to the back-bent warm front. The warm tongue of air, in phase with the PV band, is advected around the main low. These PV anomalies might be inverted into the seclusion trough with a low-level jet on its outer side. The seclusion trough is advected further around the

main low. The cold air secludes the warm anomaly and the seclusion low forms. The circulation of the main low is strong, so strong that the seclusion of cold air finally completely surrounds the warm air anomaly. A separate low centre is now seen.

The other condition is the strong upper air anomaly of PV (2.5 PVU reaching down to 600 hPa), which remains in phase with the cyclone during the seclusion process. The upper PV anomaly provides low vertical stability in the air masses taking part in the seclusion intensification. This gives favourable conditions for interaction between the upper air PV anomaly and the PV anomalies contained in the low-level warm anomaly. Indeed, a mesoscale streamer of PV (diameter 250 km) is being stretched down from the upper anomaly within six hours and acts together the anomalies below. In this way the seclusion low and the low-level jet is strengthened and both the vertical and horizontal scale of the jet is increased (core at 850 hPa, horizontal scale $\sim$250 km). Without release of latent heat, no seclusion or seclusion intensification takes place, and the frontal structure takes form of an ordinary occlusion. The winds at the surface are much weaker, maximum geostrophic winds are reduced by 50%.

From the papers of Hoskins (1990) and Thorncroft et al. (1993) it could be indicated that cyclone life cycles according to the Shapiro/Keyser model is connected to planetary-scale flows with small meridional barotropic shear. In the present case the planetary-scale meridional shear seems to be small (not shown), however, the diabatic heating is necessary to complete the seclusion. Not all cyclones with a seclusion process give a seclusion intensification. In favour of such a rapid development is probably a large displacement speed of the developing cyclone. In this way the precipitation rates will be high and the effect of latent heat relatively large. The saturated ascent ahead of the low reduces the stability and increases the Rossby height. In this way the vertical coupling is high, and a fast mesoscale development, like the seclusion intensification, might case place.

## 8. Acknowledgement

The author would like to express his appreciation for the valuable assistance made by Mr. F. Cleveland, Mr. A. Foss, Mrs. C. Ohm, Dr. N. G. Kvamstø and Ass. Prof. E. Raustein. This work has received support from the Norwegian Super Computing Committee (TRU) through a grant of computing time.

## REFERENCES

Andersen, P. 1978. On the development and structure of the rolled-up and the back-bent occlusion. *Meteorologiske Annaler, vol. 7, no. 4.* The Norwegian Meteorological Institute.

Aune, B. and Harstveit, K. 1992. The storm of 1 January 1992. *Report No. 23 1992.* Climate Department, The Norwegian Meteorological Institute, Oslo, Norway.

Bergeron, T. 1949. De tropiska orkanernas problem. *Svenska Fysikersamfundets publikation Kosmos* **27** (in Swedish).

Bergeron, T. 1954. Reviews of tropical hurricanes. *Quart. J. Roy. Meteor. Soc.* **80**, 131–164.

Breivik, L. A., Kristjansson, J. E., Midtbø, K. H., Røsting, B. and Sunde, J. 1992. *Simulation of the 1 January 1992 North Atlantic Storm.* Tech. Rep. no. 99, The Norwegian Meteorological Institute, Oslo, Norway.

Chromow, S. V. and Koncek, N. 1940. *Einführung in die synoptische Wetteranalyse.* Verlag von Julius Springer, Wien, 1940. German version by G. Swoboda.

Davis, C. A., Stoelinga, M. T. and Kuo, Y.-H. 1993. The integrated effect of condensation in numerical simulations of extratropical cyclogenesis. *Mon. Wea. Rev.* **17**, 2309–2330.

Del'Osso, L. and Klinker, E. 1994. Numerical experiments on the ERICA IOP-4 case and diagnosis of physical processes. The Life Cycle of Extratropical Cyclones. Vol. II, 169–174. Eds. S. Grønås, M. A. Shapiro. *Proceedings of an International Symposium.* Geophysical Institute, University of Bergen.

Godske, C. L., Bergeron, T., Bjerknes, J. and Bundgaard, R. C. 1957. *Dynamic meteorology and weather forecasting.* Amer. Met. Soc., Boston.

Grønås, S. and Hellevik, O. E. 1982. *A limited area prediction model at the Norwegian Meteorological Institute.* Techn. Rep. no. 61. The Norwegian Meteorological Institute.

Grønås, S. and Midtbø, K. H. 1987. Operational multivariate analyses by successive corrections. *Short- and medium-range numerical weather prediction,* ed.



Tellus A/47/5:1-16

T. Matsuno. Special Volume of the J. Meteor. Soc. Japan, 61–74.

Grønås, S., Foss, A. and Lystad, M. 1987. Numerical simulations on polar lows in the Norwegian Sea. *Tellus* **39A**, 334–353.

Grønås, S., Kvamstø, N. G. and Raustein, E. 1994. Numerical simulations of the Northern German Storm of 27–28 August 1989. *Tellus* **46A**, 635–650.

Hoskins, B. J. 1990. Theory of extratropical cyclones. Extratropical cyclones. *The Eric Palmén Memorial Volume*, eds.: C. W. Newton and E. O. Holopainen, pp. 64–79. Amer. Met. Soc., Boston.

Hoskins, B. J., McIntyre, M. E. and Robertson, A. W. 1985. On the use and significance of isentropic potential vorticity maps. *Quart. J. Roy. Meteor. Soc.* **111**, 877–946.

Kristjansson, J. E. 1990. Model simulations of an intense meso-beta scale cyclone. The role of condensation parameterization. *Tellus* **42A**, 78–91.

Kuo, Y.-H. and Reed, R. J. 1988. Numerical simulation of an explosive deepening cyclone in the eastern Pacific. *Mon. Wea. Rev.* **116**, 2081–2105.

Kuo, Y.-H., Reed, R. J. and Low-Nam, 1992. Thermal structure and airflow in a model simulation of an occluded marine cyclone. *Mon. Wea. Rev.* **120**, 2280–2297.

Neiman, P. J., Shapiro, M. A. and Fedor, L. F. 1993. The life cycle of an extratropical marine cyclone. Part I: Frontal-cyclone evolution and thermodynamic air-sea interaction. *Mon. Wea. Rev.* **121**, 2153–2176.

Neiman, P. J. and Shapiro, M. A. 1993. The life cycle of an extratropical marine cyclone. Part II: Mesoscale structure and diagnostics. *Mon. Wea. Rev.* **121**, 2177–2199.

Nordeng, T. E. 1986. *Parameterization of physical processes in a 3-dimensional numerical weather prediction model.* Technical Report no. 65. The Norwegian Meteorological Institute, Oslo, Norway.

Schär, C. J. 1989. *Dynamische aspeckte der aussertropischen zyklogenese. Theorie und numerische simulation im limit der balancierten strömungssysteme.* Dissertation No. 8845 der Eidgenössischen Technischen Hochschule, Zürich, 241 pp.

Schär, C. and Wernli, H. 1992. Structure and evolution of an isolated semi-geostrophic cyclone. *Quart. J. Roy. Met. Soc.* **119**, 57–90.

Scherhag, R. 1969. *Die "gewundene" Okklusion.* Beilage zur Berliner Wetterkarte. 43/69, SO 13/69.

Shapiro, M. A. and Keyser, D. 1990. Fronts, jet steams, and the tropopause. Extratropical cyclones. *The Erik Palmén Memorial Volume*, eds.: C. W. Newton and E. O. Holopainen, pp. 167–191. Amer. Met. Soc., Boston.

Shutts, G. J. 1990. Dynamical aspects of the October storm 1987: a study of a successful fine-mesh simulation. *Quart. J. Roy. Met. Soc.* **116**, 1315–1347.

Sundqvist, H., Berge, E. and Kristjansson, J. E. 1989. Condensation and cloud parameterization studies with a mesoscale NWP model. *Mon. Wea. Rev.* **117**, 1641–1657.

Thorpe, A. J. and Clough, S. A. 1991. Mesoscale dynamics of fronts. Structures described by dropsoundings in Fronts 87. *Quart. J. Roy. Met. Soc.* **117**, 903–941.

Thorncroft, C. D., Hoskins, B. J. and McIntyre, M. E. 1993. Two paradigms of baroclinic-wave life cycle behavior. *Quart. J. Roy. Met. Soc.* **119**, 17–55.

Uccellini, L. W. 1990. Processes contributing to the rapid development of Extratropical Cyclones. *The Eric Palmén Memorial Volume*, eds. C. W. Newton and E. O. Holopainen, pp. 81–105. Amer. Met. Soc., Boston.